WATER RESOURCES RESEARCH, VOL. 46, W07509, doi:10.1029/2009WR008568, 2010

Spatial distribution of imperviousness and the space-time variability of rainfall, runoff generation, and routing

Alfonso I. Mejía[1] and Glenn E. Moglen[2]

Received 26 August 2009; revised 22 December 2009; accepted 23 February 2010; published 10 July 2010.

[1] We study the relationship between the spatial distribution of imperviousness and the space-time variability of rainfall, runoff generation, and hydrologic response. For this study we follow an analytical framework that is able to represent space-time variability and use it to determine relationships for quantities commonly used in hydrology, for example, the amount of rainfall excess, the total runoff from a storm, the runoff ratio of developed land use to undeveloped land use, and the mean time and variance of the runoff time. The relationships are derived such that the space-time variability of rainfall, runoff, and the hydrologic response, and their relative importance, can be identified and compared. In addition, the method allows the separation of pervious and impervious contributions to runoff and the estimation of their relative influence on the hydrologic response. We illustrate the estimation of the relationships from available data and apply them to two cases. In the first case, the space-time variability of rainfall and its interaction with impervious cover is investigated. In the second case, we examine the impacts of the imperviousness pattern on runoff relationships. We find that the imperviousness and rainfall pattern can interact to either increase or decrease the average amount of rainfall excess. We also find that the influence of pervious and impervious contributions on the response can depend on the form of the overall imperviousness pattern. The proposed framework can be a useful tool for identifying the importance of different space-time hydrologic components in mixed pervious-impervious landscapes.

Citation: Mejía, A. I., and G. E. Moglen (2010), Spatial distribution of imperviousness and the space-time variability of rainfall, runoff generation, and routing, *Water Resour. Res.*, *46*, W07509, doi:10.1029/2009WR008568.

1. Introduction

[2] The increase of suburban growth, often referred to as sprawl, and its impact on water resources is becoming an important concern [*Schueler*, 1994; *Johnson*, 2001; *McCuen*, 2003; *DeFries and Eshleman*, 2004; *Environmental Protection Agency* (*EPA*), 2004; *U.S. Environmental Protection Agency* (*EPA*), 2006; *Irwin and Bockstael*, 2007; *Moglen*, 2009]. In the United States, for example, urban sprawl has led several states to consider and implement new zoning regulations [*EPA*, 2004; *U.S. EPA*, 2006; *Irwin and Bockstael*, 2007]. A distinctive characteristic of sprawl is the spreading of impervious cover throughout the land surface, producing areas characterized by a mixed pervious and impervious land use. These mixed land use areas tend to have a relatively small population density but sufficient amounts of imperviousness from roads, rooftops, parking lots, and other urban surfaces to cause environmental impacts [*Leopold*, 1968; *Schueler*, 1994; *Johnson*, 2001; *Morgan and Cushman*, 2005; *Walsh et al.*, 2005]. To mitigate some the impacts of sprawl, new zoning regulations tend to emphasize the clustering of imperviousness [*EPA*, 2004; *U.S. EPA*, 2006]. The clustering of imperviousness is becoming a popular policy instrument because it is thought to be beneficial to the environment and particularly to water resources [*EPA*, 2004; *U.S. EPA*, 2006]. The benefits to water resources are often addressed qualitatively or, when quantified, they are done in detachment from hydrologic processes, the space-time variability of these processes, and watershed scale. Watershed scale is understood as the size of the watershed, and in this case it is taken as encompassing the possible range of drainage areas from channel initiation to the main watershed outlet within a single watershed.

[3] The concept that the spatial form of imperviousness (i.e., clustering or spreading) can be regulated and managed to reduce impacts led us to consider how the spatial distribution of imperviousness across the watershed interacts with the space-time variability of hydrologic processes. Normally, imperviousness is lumped into a few categories (e.g., high- and low-density residential) and analyzed at the hillslope scale because this is typically the scale of individual residential development. Thus, we decided to study this interaction by including the space-time variability of rainfall, runoff generation, and hydrologic response. The space-time variability of hydrologic processes at the watershed scale has been studied and analyzed for a range of conditions [*Rinaldo et al.*, 1991; *Woods and Sivapalan*, 1999; *Menabde and Sivapalan*, 2001; *Segond et al.*, 2007; *Nicótina et al.*, 2008]. For instance, the role of the space-time pattern of rainfall on hydrologic response has been investigated by various researchers [*Menabde and Sivapalan*, 2001; *Segond*

[1]Department of Civil and Environmental Engineering, University of Maryland, College Park, Maryland, USA.
[2]Department of Civil and Environmental Engineering, Virginia Tech, Falls Church, Virginia, USA.

0043-1397/10/2009WR008568

et al., 2007; *Nicótina et al.*, 2008]. Variability in the hydrologic response has been studied extensively using the theory of the geomorphologic unit hydrograph [*Rinaldo et al.*, 1991; *Saco and Kumar*, 2004; *Moussa*, 2008]. The space-time variability of data and processes for urbanized watersheds has been studied little and typically is done as an indirect consequence of the requirements of rainfall-runoff models where the relationship between the different sources of variability cannot be identified as clearly or is difficult to decipher [*Niehoff et al.*, 2002; *Hundecha and Bárdossy*, 2004].

[4] An attractive approach for investigating the behavior of the space-time variability of hydrologic processes is to use fully distributed physical models. The application of distributed models is complicated by the uncertainty of required input data, the identifiability of parameters, and the need to select the proper level of model complexity [*Grayson et al.*, 1992]. As an alternative, and to support the development of more detailed models, *Woods and Sivapalan* [1999] proposed an analytical framework to synthesize the complexity of space-time variations in hydrologic data and processes.

[5] For this investigation we build on the analytical framework of *Woods and Sivapalan* [1999] by including the spatial distribution of imperviousness. The framework is based on the simplifying assumption of the space-time separability of rainfall and the runoff generation function [*Eagleson*, 1967; *Sivapalan and Wood*, 1987; *Woods and Sivapalan*, 1999], as well as any specific assumptions made about the hydrologic processes. The method allows the analytical expression of the space-time variability of rainfall, runoff, and hydrologic response such that these space-time variabilities can be tracked and compared when estimating useful hydrologic relationships [*Woods and Sivapalan*, 1999]. The method in this case is also used to gain insight into the role of the imperviousness pattern by providing a basis for comparing scenarios and identifying dominant controls. To present the method, we first identify and describe the space-time variability of the data and processes. We then develop the analytical approach and determine hydrologic relationships based on the space-time variability identified. Finally, we use the relationships to study the role of the spatial distribution of imperviousness.

2. Space-Time Variabilities from Pervious and Impervious Areas

[6] We are interested in relating the space-time components of rainfall, runoff, and the routing process to the spatial distribution of imperviousness. To achieve this goal, we express the space-time variability of runoff, $R(x,y,t)$ [L T^{-1}], with an equation useful to define the generated runoff into pervious and impervious contributions. This definition allows us to track these two sources of runoff and compare their relative contributions as shown later. Specifically we have the following:

$$R(x,y,t) = P(x,y,t)W(x,y,t)[1 - I(x,y)] + P(x,y,t)I(x,y). \quad (1)$$

The first term in (1) is the runoff generated from pervious areas, $R(x,y,t)_p$, where saturation or infiltration excess occurs, and the last term is the runoff from impervious areas or the impervious fraction of individual cells, $R(x,y,t)_i$. In the remainder of this paper, we use the subscript p to refer to pervious areas and i for impervious ones. $P(x,y,t)$ [L T^{-1}] is the rainfall field, $W(x,y,t)$ is the runoff generation function field, and $I(x,y)$ is the imperviousness pattern and assumes values specified in section 2.1. The x, y coordinates identify the location where the variable is being estimated and t is the time during the storm event. We discretize the watershed into a grid of regular squares such that x, y represents the different cells in the grid. $W(x,y,t)$ is the fraction of rainfall that becomes runoff at a given cell; it can take a value ranging from 0 to 1, where 0 means all the rainfall on a given x, y cell at time t infiltrates and 1 means all the rainfall becomes runoff. In practice, the runoff generation function can be determined by various methods, such as an infiltration equation, a topographic index, or a curve number, as long as the runoff is properly normalized to be between 0 and 1 [*Philip*, 1960; *Beven and Kirkby*, 1979; *National Resources Conservation Service* (*NRCS*), 1986]. Equation (1) assumes all the rainfall falling on impervious areas becomes runoff, which can be a reasonable assumption for connected imperviousness. To study how the space-time variability of $P(x,y,t)$, $W(x,y,t)$, and the spatial $I(x,y)$ pattern contribute to runoff, we assume they can be separated into multiplicative space and time processes [*Eagleson*, 1967; *Woods and Sivapalan*, 1999]. The way these processes are separated is discussed in section 2.1.

2.1. Rainfall and Runoff Generation Variability

[7] Using the separability assumption, the rainfall field $P(x,y,t)$ can be represented by independent space, $P_t(x,y)$ [ ], and time variations, $P_{x,y}(t)$ [L T^{-1}], such that [*Eagleson*, 1967; *Woods and Sivapalan*, 1999]

$$P(x,y,t) = P_{x,y}(t)P_t(x,y), \quad (2)$$

where $P_{x,y}(t)$ is the instantaneous areal-averaged rainfall and equal to

$$P_{x,y}(t) = \frac{1}{A}\iint_A P(x,y,t)\,dx\,dy, \quad (3)$$

where A [L^2] is the drainage area of the watershed under consideration, which results from integrating the local area of each x,y cell over the watershed; $P_t(x,y)$ is the spatial pattern of rainfall determined by dividing the total rainfall falling on every grid cell in the watershed by the total average rainfall falling over the entire watershed for a given storm event such that

$$P_t(x,y) = \frac{\int_0^{T_s} P(x,y,t)\,dt}{\int_0^{T_s} P_{x,y}(t)\,dt}, \quad (4)$$

where T_s [T] is the storm duration, assuming the time at the start of the storm is 0. A similar assumption is made for the space and time variations of the runoff generation function such that

$$W(x,y,t) = W_{x,y}(t)W_t(x,y), \quad (5)$$

where $W_{x,y}(t)$ is the areal-averaged value of W, determined as

$$W_{x,y}(t) = \frac{1}{A}\iint_A W(x,y,t)\,dx\,dy, \tag{6}$$

and $W_t(x,y)$ is the spatial pattern of runoff generation function and estimated similarly to (4) as follows:

$$W_t(x,y) = \frac{\int_0^{T_s} W(x,y,t)\,dt}{\int_0^{T_s} W_{x,y}(t)\,dt}. \tag{7}$$

[8] It is important to notice that W is amenable to the representation of impervious data derived from remote sensing [*Homer et al.*, 2007]. These data represent the amount of imperviousness on each grid cell as a continuous value between 0 and 1. Assuming the imperviousness pattern is constant in time, the space and time variations for $I(x,y)$ are as follows:

$$I_t(x,y) = \frac{I(x,y)}{f} \tag{8}$$

and

$$I_{x,y}(t) = f, \tag{9}$$

where f is the total fraction of imperviousness in the watershed and equal to

$$f = \frac{1}{A}\iint_A I(x,y)\,dx\,dy. \tag{10}$$

Even though $I(x,y)$ is only a function of space, we retain the notation in equation (8) to refer to the normalized $I(x,y)$ value.

2.2. Runoff Routing Variability

[9] The variability associated with the hydrologic response is quantified using the mean and variance of the travel times assuming a Geomorphic Instantaneous Unit Hydrograph (GIUH) approach [*Rinaldo and Rodríguez-Iturbe*, 1996; *Rodríguez-Iturbe and Rinaldo*, 1997]. This approach has been shown to be useful for suburban watersheds [*Olivera and Maidment*, 1999; *Smith et al.*, 2005]. The estimation of the response to the rainfall excess generated over a hillslope in a location k along the stream network can be expressed as follows [*Rinaldo and Rodríguez-Iturbe*, 1996]:

$$Q_k(t) = \sum_{\gamma\in\Gamma}\int_0^t R_{x,y}(\tau)*p(\gamma)f_\gamma(t-\tau)\,d\tau, \tag{11}$$

where $R_{x,y}(t)$ is the time component of the runoff generation process. The exact way in which $R_{x,y}(t)$ is estimated is shown in section 3. The variable $p(\gamma)$ is the likelihood of a given path γ to carry water to the outlet, and $f_\gamma(t)$ is the path response function [*Rinaldo and Rodríguez-Iturbe*, 1996]. Every cell in the discretized watershed, or upstream from k, is assumed to be a possible path. We assume $f_\gamma(t)$ to include both hillslope and channel sections of a path and to be represented by an inverse Gaussian probability density function [*Mesa and Mifflin*, 1986; *Rinaldo and Rodríguez-Iturbe*, 1996]. We assume $p(\gamma)$ to be equal to

$$p(\gamma) = \frac{R_t(x,y)}{\iint_A R_t(x,y)\,dx\,dy}, \tag{12}$$

where $R_t(x,y)$ is the spatial pattern of runoff and its estimation is shown in section 3. Equation (12) is divided by the total value of $R_t(x,y)$ to ensure the sum of all $p(\gamma)$ is 1. In (12) it is assumed that the likelihood of a path is proportional to the time-averaged fraction of runoff generated at a given location in the watershed. While other expressions have been used for (12) [*Rinaldo et al.*, 1991; *Olivera and Maidment*, 1999; *Nicótina et al.*, 2008], we chose this one because it can include the effects of imperviousness in a simple but direct manner. We also assume that the trajectory of both pervious and impervious paths follows the topographic gradient. In the absence of detailed stormwater data, this simplification seems reasonable. To determine the mean and variance of the travel times we use the equations previously derived by *Rinaldo et al.* [1991], and we track the runoff from pervious and impervious cells to separate the mean and variance of the travel times into pervious and impervious times. This separation is a simple way to measure the relative effects of pervious and impervious areas on the response. The mean travel time for impervious surfaces is determined as follows [*Rinaldo et al.*, 1991; *Saco and Kumar*, 2002]:

$$E[T_b]_i = \sum_{\gamma\in\Gamma_i} p(\gamma)\frac{L_\gamma}{u_\gamma}, \tag{13}$$

where T_b [T] is the travel time after accounting for all the possible paths in the watershed; L_γ [L] and u_γ [L/T] are the path-dependent length and wave celerity, respectively; and Γ is the set of all possible paths. The subscript i in equation (13) indicates runoff that originated from impervious areas; it can be replaced by the subscript p to obtain an expression for pervious surfaces. The total expected travel time for the watershed is

$$E[T_b] = E[T_b]_i + E[T_b]_p. \tag{14}$$

To estimate the variance of the travel times we use the following expression but separate the variance according to runoff from pervious and impervious surfaces:

$$\mathrm{Var}(T_b)_i = 2\sum_{\gamma\in\Gamma_i} p(\gamma)\frac{L_\gamma D_\gamma}{u_\gamma^3} + \sum_{\gamma\in\Gamma_i} p(\gamma)\left(\frac{L_\gamma}{u_\gamma}\right)^2 - \left[\sum_{\gamma\in\Gamma_i} p(\gamma)\frac{L_\gamma}{u_\gamma}\right]^2 - \left[\sum_{\gamma\in\Gamma_i} p(\gamma)\frac{L_\gamma}{u_\gamma}\right]\left[\sum_{\gamma\in\Gamma_p} p(\gamma)\frac{L_\gamma}{u_\gamma}\right], \tag{15}$$

Figure 1. (a) Spatial distribution of rainfall (cm/h) for the 21 March 2001 storm; (b) $P_t(x,y)$ pattern, obtained using equation (6); and (c) map illustrating the NW Branch watershed, including the stream network and the imperviousness pattern. The black dot indicates the location of the main outlet.

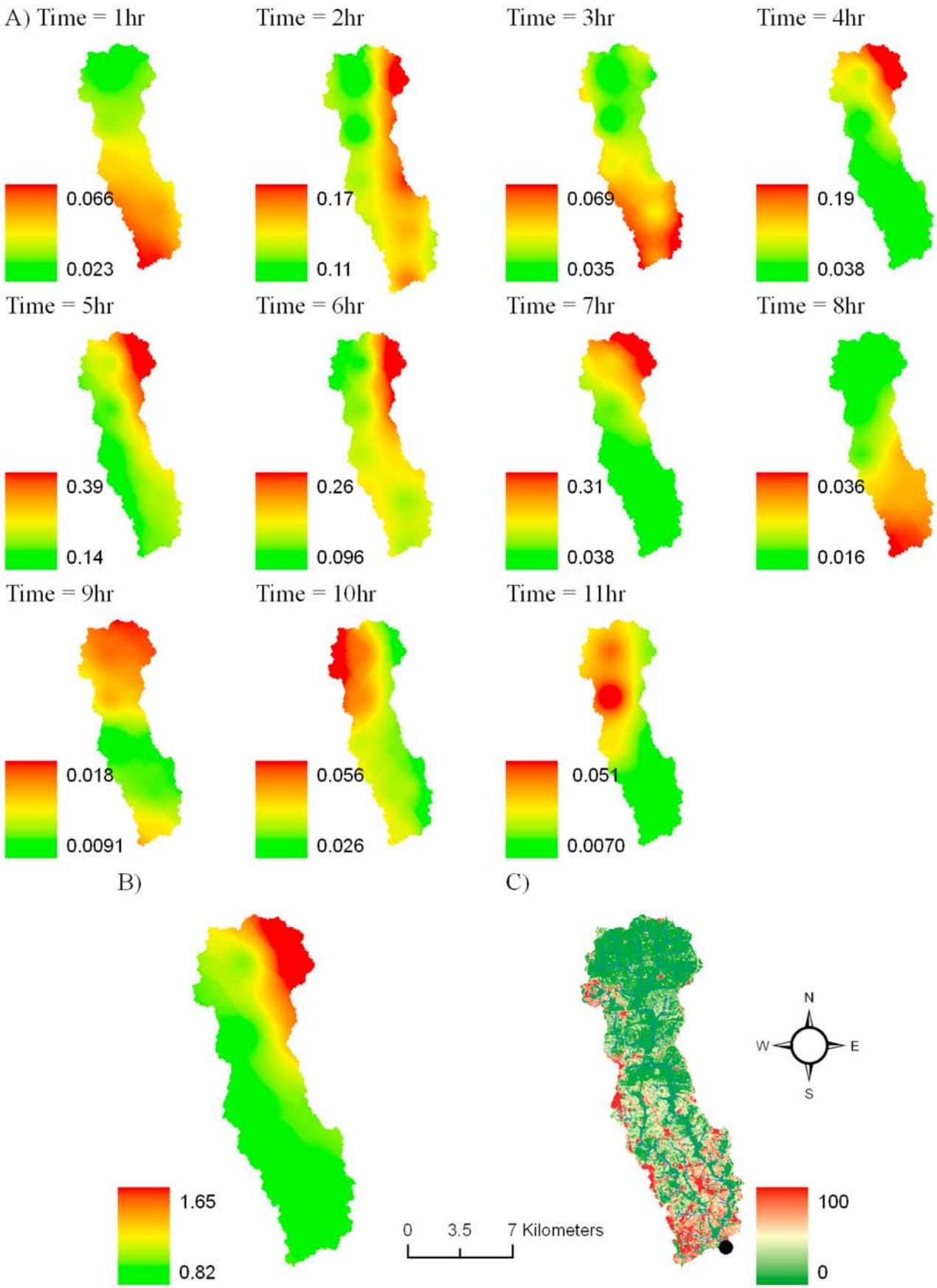
A) Time = 1hr
0.066
0.023
Time = 2hr
0.17
0.11
Time = 3hr
0.069
0.035
Time = 4hr
0.19
0.038
Time = 5hr
0.39
0.14
Time = 6hr
0.26
0.096
Time = 7hr
0.31
0.038
Time = 8hr
0.036
0.016
Time = 9hr
0.018
0.0091
Time = 10hr
0.056
0.026
Time = 11hr
0.051
0.0070
B)
C)
1.65
0.82
0 3.5 7 Kilometers
N
W
E
S
100
0

Figure 1

where $\mathrm{Var}(T_b)_i$ indicates that equation (15) is for the impervious portion of the watershed and D_γ [L^2/T] is the path-dependent dispersion coefficient. By substituting the subscript i above for p, a similar expression for the variance of the pervious portion of the watershed, $\mathrm{Var}(T_b)_p$, can be obtained. The variance of the travel times measures the spread of the response [*Rinaldo et al.*, 1991; *Saco and Kumar*, 2004]. The usefulness of the variance is demonstrated in section 5.2, where it is used to define the peakedness of the response. Additionally, it is possible to separate the terms in (15) into geomorphologic, kinematic, and hydrodynamic dispersions, which have been shown to be very useful for studying the response of watersheds under various conditions [*Rinaldo et al.*, 1991; *Saco and Kumar*, 2002, 2004; *Nicótina et al.*, 2008]. The total variance of the travel times from pervious and impervious surfaces is as follows:

$$\mathrm{Var}(T_b) = \mathrm{Var}(T_b)_i + \mathrm{Var}(T_b)_p. \tag{16}$$

Equations (14) and (16) can be compared to a time of concentration and the response duration, respectively [*Woods and Sivapalan*, 1999; *Saco and Kumar*, 2004]. They are useful because they provide a simple analytical way of explaining the influence of imperviousness on the hydrologic response.

3. Data

[10] To illustrate the application of the proposed method we selected the Northwest Branch of the Anacostia River watershed (NW Branch) located in the Maryland Piedmont physiographic region. The watershed is characterized by a suburban pattern where the main land use categories are pervious forested and grassed areas and impervious residential developments with mixtures of pervious and impervious areas. The watershed has a drainage area of 124 km^2, of which approximately 17% is impervious. The density of imperviousness in the watershed tends to increase as one moves from the most upstream areas toward the overall watershed outlet. Figure 1c illustrates the imperviousness distribution in the watershed. To represent imperviousness we used the National Land Cover Database (NLCD) 2001, which is derived from remotely sensed data [*U.S. Geological Survey* (*USGS*), 2008b]. For the rainfall we used Next Generation Weather Radar (NEXRAD) Stage III radar data [*NOAA*, 2008]. The NLDC data represent imperviousness using a grid scheme with cells having values that range from 0 to 1, where 0 is a fully pervious cell and 1 is fully impervious. The NEXRAD data have a time resolution of 1 h and a space resolution of approximately 4 km. To interpolate the rainfall, we used an inverse squared distance weighting scheme, which was found to be applicable [*Smith et al.*, 2005]. The digital elevation model data were obtained from the USGS [*USGS*, 2008a]. Figure 1a shows the storm event chosen to illustrate the application of the method. Figure 1b is the spatial pattern of $P_t(x,y)$, obtained using equation (4). The spatial pattern in Figure 1b resembles several of the individual hourly spatial patterns in Figure 1a. It resembles the patterns that contribute the most rainfall and it captures the main spatial characteristics of the storm event. For this storm, most of the rainfall falls on the upper areas of the watershed relative to the areas near the main outlet.

[11] To estimate the runoff generation function $W(x,y,t)$, we used a simple event model (e.g., for a practical application see *Troch et al.* [1994]). The model uses a topographic index and Philip's infiltration equation to estimate the generated runoff during a storm event on a cell by cell basis [*Philip*, 1960; *Beven and Kirkby*, 1979]. The generated runoff on cell x,y at time t is normalized by the rain falling on the cell to obtain a value between 0 and 1 for $W(x,y,t)$. Additionally, the imperviousness in the NW Branch watershed is mostly connected and the effects from best management practices are minimal as assumed by equation (1). The parameters used to determine the runoff generation function in equation (5) and the mean and variance of the travel times in equations (13) and (15), respectively, were obtained from a previous modeling study [*Mejía*, 2009].

4. Space-Time Relationships for Pervious-Impervious Areas

[12] In this section we use the separation and estimation of variations in rainfall, runoff, and routing presented in section 2 to develop several hydrologic relationships. The relationships estimated are (1) the instantaneous rainfall excess, (2) the storm-averaged watershed rainfall excess, (3) the ratio of instantaneous rainfall excess, (4) the ratio of storm-averaged watershed rainfall excess, and (5) the mean and variance of the watershed runoff time. The ratio in measures 3 and 4 is the runoff from the pervious-impervious land use to the runoff assuming a fully pervious land use. The estimation of these five relationships is presented in sections 4.1–4.5 based on the data for the NW Branch watershed.

4.1. Instantaneous Rainfall Excess

[13] To determine the instantaneous rainfall excess, $R_{x,y}(t)$, we use the areal-averaged value of equation (1) as follows:

$$R_{x,y}(t) = \frac{1}{A}\iint_A P(x,y,t)W(x,y,t)[1 - I(x,y)]\,dx\,dy + \frac{1}{A}\iint_A P(x,y,t)I(x,y)\,dx\,dy. \tag{17}$$

Using the separability assumption for $P(x,y,t)$ and $W(x,y,t)$ defined in equations (2) and (5), respectively, letting $W(x, y, t)[1 - I(x, y)]$ be equal to a new variable $W^*(x,y,t)$, and by taking out the time-dependent terms from the integrals, we find

$$R_{x,y}(t) = P_{x,y}(t)W^*_{x,y}(t)\frac{1}{A}\iint_A P_t(x,y)W^*_t(x,y)\,dx\,dy + P_{x,y}(t)f\frac{1}{A}\iint_A P_t(x,y)I_t(x,y)\,dx\,dy, \tag{18}$$

where W^* is the amount of runoff that can be generated on the pervious portion of an individual grid cell with a mixed land use. Using $\mathrm{Cov}(x,y)=E[xy] - E[x]E[y]$, and by noting that the integrals in (18) can be interpreted as the expected value of two random variables, equation (18) can be written as follows:

$$R_{x,y}(t) = R_{x,y}(t)_p + R_{x,y}(t)_i, \tag{19}$$

Table 1. Estimates of the Terms in Equations (29) and (30) for the Overall Watershed

Terms in Equations (29) and (30)	Value
$P_{x,y,t}$ (cm/h)	0.201
$W^*_{x,y,t}$	0.293
$P_{x,y,t}W^*_{x,y,t}$ (cm/h)	0.0588
$P_{x,y,t}f$ (cm/h)	0.0351
Cov[$P_t(x, y)$, $W_t^*(x, y)$]	−0.0102
Cov[$P_{x,y}(t)$, $W^*_{x,y}(t)$] (cm/h)	-1.15×10^{-4}
Cov[$P_t(x, y)$, $I_t(x, y)$]	−0.0771
$(R_{x,y,t})_p$ (cm/h)	0.0583
$(R_{x,y,t})_i$ (cm/h)	0.0324

where

$$R_{x,y}(t)_p = P_{x,y}(t)W^*_{x,y}(t)\{1 + \mathrm{Cov}[P_t(x,y), W_t^*(x,y)]\} \quad (20)$$

and

$$R_{x,y}(t)_i = P_{x,y}(t)f\{1 + \mathrm{Cov}[P_t(x,y), I_t(x,y)]\}, \quad (21)$$

because the areal integrals of $P_t(x,y)$, $W_t(x,y)$, and $I_t(x,y)$ are unity by the definitions given in section 2.1. The illustration of equations (20) and (21) is shown in Figure 2. In Figure 2 the rainfall excess owing to pervious areas is larger than that from impervious areas. Also, the value of $W^*_{x,y}(t)$ remains nearly constant in Figure 2, indicating the time variations in $R_{x,y}(t)$ for pervious areas are due to the time variation in rainfall, because we found Cov[$P_t(x, y)$,W_t^* (x, y)] to be small, approximately −0.01. However, we found Cov[$P_t(x,y)$, $I_t(x,y)$] to be equal to −0.08, which is comparable, as a reference, to the areal reduction amount suggested for a 12 h storm over an 180 km^2 watershed [*National Weather Service* (*NWS*), 1961], suggesting that the interaction between rainfall and the imperviousness pattern can have a significant effect on the rainfall excess from impervious areas. The impact of Cov[$P_t(x,y)$,$I_t(x,y)$] on the generated runoff from impervious areas is explored further in section 5.

4.2. Storm-Averaged Watershed Rainfall Excess

[14] The storm-averaged watershed rainfall excess is estimated from equations (20) and (21) by integrating the rainfall excess over the storm duration as follows [*Woods and Sivapalan*, 1999]:

$$R_{x,y,t} = \frac{1}{T_s}\int_o^{T_s} R_{x,y}(t)\,dt. \quad (22)$$

For pervious and impervious areas equations (20) and (21), respectively, are substituted into (22), yielding the following expression:

$$R_{x,y,t} = \frac{1}{T_s}\int_o^{T_s} P_{x,y}(t)W^*_{x,y}(t)\{1 + \mathrm{Cov}[P_t(x,y), W_t^*(x,y)]\}\,dt + \frac{1}{T_s}\int_o^{T_s} P_{x,y}(t)I_{x,y}(t)\{1 + \mathrm{Cov}[P_t(x,y), I_t(x,y)]\}\,dt. \quad (23)$$

The time-independent terms can be taken out of the integrals in (23). The terms $T_s^{-1}\int_o^{T_s}P_{x,y}(t)W^*_{x,y}(t)\,dt$ and $T_s^{-1}\int_o^{T_s}P_{x,y}(t)$ $I_{x,y}(t)\,dt$ can both be interpreted as the expected value of two random variables, and using the relationship between the covariance and the expected value of two random variables, the expression in (23) can be written as

$$R_{x,y,t} = (R_{x,y,t})_p + (R_{x,y,t})_i, \quad (24)$$

where

$$(R_{x,y,t})_p = \{1 + \mathrm{Cov}[P_t(x,y), W_t^*(x,y)]\}\{P_{x,y,t}W^*_{x,y,t} + \mathrm{Cov}[P_{x,y}(t), W^*_{x,y}(t)]\} \quad (25)$$

and

$$(R_{x,y,t})_i = \{1 + \mathrm{Cov}[P_t(x,y), I_t(x,y)]\}P_{x,y,t}f. \quad (26)$$

Equations (25) and (26) are the averaged runoff generated from pervious and impervious areas, respectively.

[15] The estimated value of the terms in (25) and (26) for the main watershed in NW Branch is included in Table 1. The storm-averaged watershed rainfall excess for the pervious areas is approximately equal to 0.058 cm/h and for the impervious areas 0.032 cm/h, which was expected since the rainfall excess from pervious areas was larger than from impervious areas as illustrated in Figure 2.

4.3. Instantaneous Ratio of Rainfall Excess

[16] Dividing equations (19) and (24) by the equivalent relationship for fully pervious conditions, with $I(x,y) = 0$, allows the evaluation of hydrologic responsiveness to impervious area (e.g., following the examples of *Carter* [1961] and *Anderson* [1970]). We use this to determine the instantaneous ratio of rainfall excess as follows:

$$r(x,y,t) = \frac{P(x,y,t)W^*(x,y,t) + P(x,y,t)I(x,y)}{P(x,y,t)W(x,y,t)}. \quad (27)$$

In equation (27), $W(x,y,t)$ is the runoff generation function, if we assume every cell is fully pervious. After some manipulations, for the instantaneous ratio of rainfall excess, we obtain the following expression:

$$r_{x,y}(t) = r_{x,y}(t)_p + r_{x,y}(t)_i, \quad (28)$$

where

$$r_{x,y}(t)_p = \frac{W^*_{x,y}(t)\{1 + \mathrm{Cov}[P_t(x,y), W_t^*(x,y)]\}}{W_{x,y}(t)\{1 + \mathrm{Cov}[P_t(x,y), W_t(x,y)]\}} \quad (29)$$

and

$$r_{x,y}(t)_i = \frac{f\{1 + \mathrm{Cov}[P_t(x,y), I_t(x,y)]\}}{W_{x,y}(t)\{1 + \mathrm{Cov}[P_t(x,y), W_t(x,y)]\}}. \quad (30)$$

$W_{x,y}(t)$ and $W_t(x,y)$ are the equivalent of equations (6) and (7) but assuming a fully pervious watershed. The numerators in (29) and (30) are equal to $R_{x,y}(t)_p$ and $R_{x,y}(t)_i$, respectively. The denominators in both (29) and (30) are the same and equal to $R_{x,y}(t)_{\mathrm{fp}}$, the subscript fp indicates the value is for fully pervious conditions.

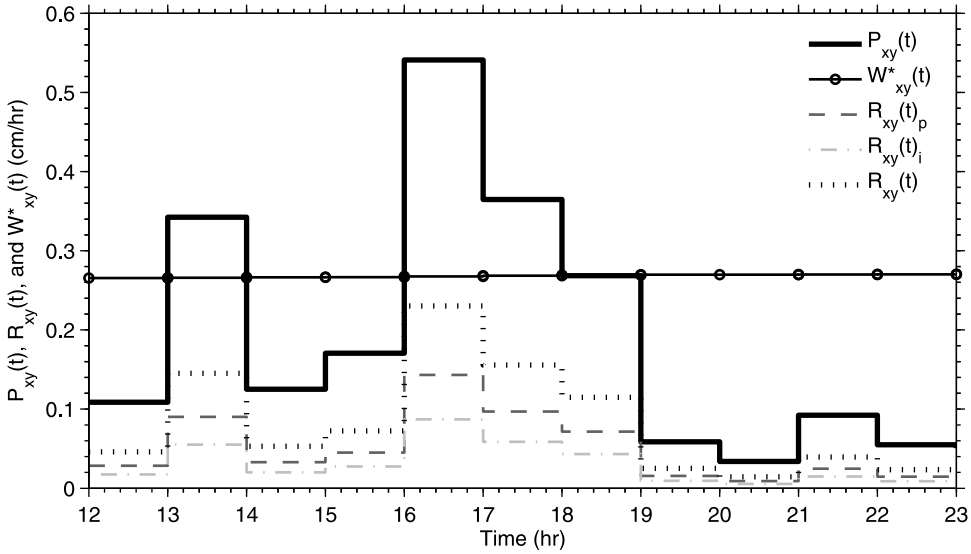

Figure 2. Illustration of the instantaneous rainfall excess, $R_{x,y}(t)$, and the separated pervious and impervious series, $R_{x,y}(t)_p$ and $R_{xy}(t)_i$, respectively. The runoff generation function, $W_{x,y}(t)$, and rainfall series, $P_{x,y}(t)$, are also shown.

[17] The estimation of equations (29) and (30) is shown in Figure 3. The rainfall excess series for fully pervious conditions decreases overall by approximately 25% when compared to the mixed pervious-impervious series. However, the ratio of rainfall excess decreases slightly for both pervious and impervious conditions. This is the case here because the pervious portions of the watershed are contributing the most runoff and only a small amount of saturated area is formed during the storm event. Notice that it is possible for the change between mixed pervious-impervious and fully pervious conditions to vary with time; this change is typically assumed constant during the storm [*Anderson*, 1970], suggesting that it is not necessarily representing the most severe change.

4.4. Storm-Averaged Ratio of Watershed Rainfall Excess

[18] For the ratio of storm-averaged rainfall excess, similarly to the way equations (29) and (30) were obtained, we start as follows:

$$r_{x,y,t} = \frac{T_s^{-1}\int_o^{T_s} R_{x,y}(t)\,dt}{T_s^{-1}\int_o^{T_s} R_{x,y}(t)_{\mathrm{fp}}dt}, \tag{31}$$

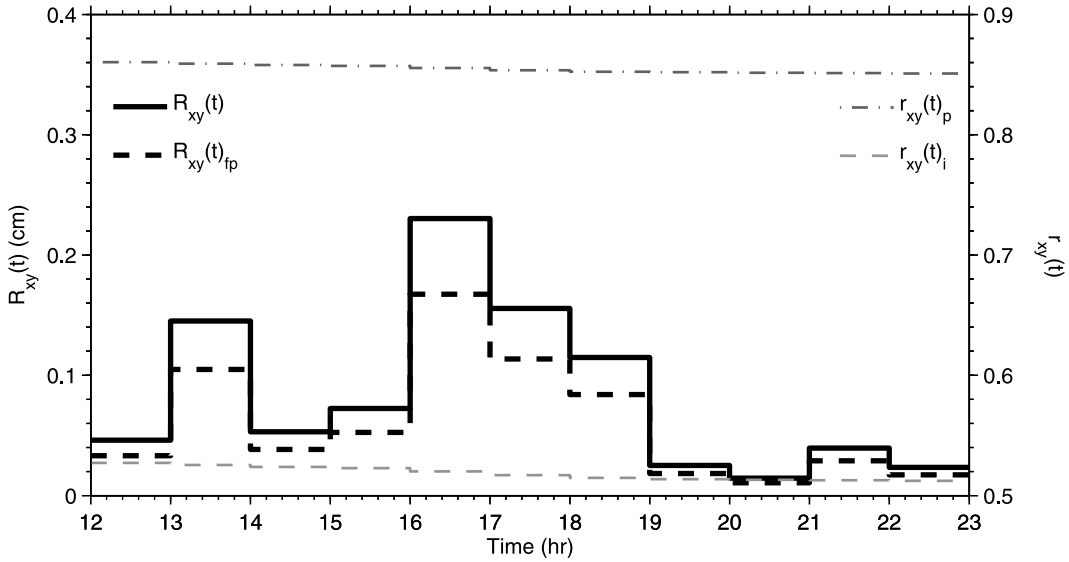

Figure 3. Illustration of the instantaneous ratio of rainfall excess for pervious and impervious areas, $r_{x,y}(t)_p$ and $r_{x,y}(t)_i$, respectively. The rainfall excess series for the pervious-impervious and the fully pervious land use conditions, $R_{x,y}(t)$ and $R_{x,y}(t)_{\mathrm{fp}}$, respectively, are also shown.

Table 2. Estimates of the Terms in Equations (37) and (38) for the Overall Watershed

Terms in Equations (37) and (38)	Value
$W_{x,y,t}$	0.34
$P_{x,y,t}W_{x,y,t}$ (cm/h)	0.0684
Cov$[P_{x,y}(t), W^*_{x,y}(t)]$ (cm/h)	-2.04×10^{-4}
Cov$[P_t(x, y), I_t(x, y)]$	−0.0771
$(r_{x,y,t})_p$	0.855
$(r_{x,y,t})_i$	0.476

where $R_{x,y}(t)_{\mathrm{fp}}$ is for a fully pervious watershed and $R_{x,y}(t)$ is for the mixed pervious-impervious land use condition. After substituting for the terms in the integrals and some manipulations, we obtain

$$r_{x,y,t} = (r_{x,y,t})_p + (r_{x,y,t})_i, \tag{32}$$

where

$$(r_{x,y,t})_p = \frac{\{1 + \mathrm{Cov}[P_t(x,y), W_t^*(x,y)]\}\{P_{x,y,t}W^*_{x,y,t} + \mathrm{Cov}[P_{x,y}(t), W^*_{x,y}(t)]\}}{\{P_{x,y,t}W_{x,y,t} + \mathrm{Cov}[P_{x,y}(t), W_{x,y}(t)]\}\{[1 + \mathrm{Cov}[P_t(x,y), W_t(x,y)]\}}$$

and

$$(r_{x,y,t})_i = \frac{\{1 + \mathrm{Cov}[P_t(x,y), I_t(x,y)]\}\{P_{x,y,t}f\}}{\{P_{x,y,t}W_{x,y,t} + \mathrm{Cov}[P_{x,y}(t), W_{x,y}(t)]\}\{[1 + \mathrm{Cov}[P_t(x,y), W_t(x,y)]\}}. \tag{34}$$

The numerators in (33) and (34) are equal to $(R_{x,y,t})_p$ and $(R_{x,y,t})_i$, respectively. The denominators are the storm-averaged value when the watershed is fully pervious, and the value is the same for (33) and (34).

[19] The estimate for the new terms in equations (33) and (34) is included in Table 2; the other terms are included in Table 1. In Table 2, the value of $r_{x,y,t}$ for the pervious areas is 0.855 instead of 1, because for the fully pervious condition some of the cells that had a fraction of impervious cover in the mixed land use condition are now fully saturated. This suggests that when impervious cover is located in areas prone to soil saturation, the generated runoff can remain approximately the same for fully pervious or mixed land use conditions. This condition can also indicate locations where runoff from imperviousness might be mitigated. For example, *Naef et al.* [2002] used similar information, together with field observations, to map different runoff mechanisms and showed how these can help manage land use changes. The sum of $(r_{x,y,t})_p$ and $(r_{x,y,t})_i$ is equal to 1.33, accounting for the impervious cells in the soil saturated areas and indicating that 36% of 1.33 is due to the impervious cover. The estimate is slightly larger than the 33% that would likely be assumed if saturated areas were not considered. This means that, if one does not account for the coincidence between imperviousness and soil saturated areas, it is possible for the increase in runoff from impervious areas to be underestimated.

4.5. Mean and Variance of the Runoff Time

[20] To estimate the mean and variance of the runoff time we assume the runoff time can be separated into two successive stages, each characterized by a holding time considered to be an independent random variable. The same holding time assumption was made by *Woods and Sivapalan* [1999] and *Rodríguez-Iturbe and Valdés* [1979]. The first stage is the time it takes for runoff to be produced, including the waiting time for rain to fall, and the second stage is the combined hillslope and channel routing times or the time for runoff to reach the outlet after its generation. The total time for water to reach the outlet, T_o, is expressed as

$$T_o = T_r + T_b, \tag{35}$$

where T_r is the holding time for rainfall excess and T_b is that for the hillslope and channel routing. Assuming the terms in (35) are independent random variables, the mean and variance of T_o are equal to the sum of the mean and variance of the individual terms, as follows:

$$E[T_o] = E[T_r] + E[T_b], \tag{36}$$

The term $E[T_b]$ is estimated using (13) and (14). To determine $E[T_r]$, we assume the distribution of T_r, f_{T_r} is defined as follows [*Woods and Sivapalan*, 1999]:

$$f_{T_r}(t) = \frac{R_{x,y}(t)}{\int_o^{T_s} R_{x,y}(t)\,dt}, \tag{37}$$

such that

$$E[T_r] = \int_0^{T_s} t f_{T_r}(t)\,dt. \tag{38}$$

After (19) is substituted into (37) and some manipulations, we arrive at the following result:

$$E[T_r] = E[T_r]_p + E[T_r]_i, \tag{39}$$

where

$$E[T_r]_p = \{1 + \mathrm{Cov}[P_t(x,y), W_t^*(x,y)]\} \times \frac{\{E[T]E[P_{x,y}(T)W^*_{x,y}(T)] + \mathrm{Cov}[T, P_{x,y}(T)W^*_{x,y}(T)]\}}{R_{x,y,t}} \tag{40}$$

and

$$E[T_r]_i = \{1 + \mathrm{Cov}[P_t(x,y)I_t(x,y)]\} \times \frac{\{E[T]E[P_{x,y}(T)f] + \mathrm{Cov}[T, P_{x,y}(T)f]\}}{R_{x,y,t}}. \tag{41}$$

The terms in (40) and (41) were defined earlier with the exception of the random variable T. We assume T is the time during the storm and that it is uniformly distributed between 0 and the total duration of the storm, T_s [*Woods and Sivapalan*, 1999]. For example, in this case $E[T]$ is 5.5 because the storm lasts 11 h.

[21] Similarly for the variance of the runoff time, assuming T_r and T_b to be independent, we have

$$\mathrm{Var}(T_o) = \mathrm{Var}(T_r) + \mathrm{Var}(T_b), \tag{42}$$

where $\mathrm{Var}(T_b)$ can be estimated using (14) and (15). To determine $\mathrm{Var}(T_r)$, we use

$$\mathrm{Var}(T_r) = E[T_r^2] - E[T_r]^2, \tag{43}$$

together with (40) and (41). The second term in (43), $E[T_r]^2$, is obtained by taking the square of (39). The term $E[T_r^2]$ is obtained by substituting t^2 into (38). After performing some additional substitutions and manipulations, we obtain the following expressions for $E[T_r^2]$:

$$E[T_r^2]_p = \{1 + \mathrm{Cov}[P_t(x,y), W_t^*(x,y)]\} \times \frac{\{E[T^2]E[P_{x,y}(T)W_{x,y}^*(T)] + \mathrm{Cov}[T^2, P_{x,y}(T)W_{x,t}^*(T)]\}}{R_{x,y,t}}, \tag{44}$$

$$E[T_r^2]_i = \{1 + \mathrm{Cov}[P_t(x,y), I_t(x,y)]\} \times \frac{\{E[T^2]E[P_{x,y}(T)f] + \mathrm{Cov}[T^2, P_{x,y}(T)f]\}}{R_{x,y,t}}. \tag{45}$$

[22] Ultimately, $\mathrm{Var}(T_r)$ is estimated by substituting (40), (41), (44), and (45) into the following relationship, which is another way of expressing (43):

$$\mathrm{Var}(T_r) = \{E[T_r^2]_p + E[T_r]_p^2\} + \{E[T_r^2]_i + E[T_r]_i^2\} + 2E[T_r]_p E[T_r]_i. \tag{46}$$

To separate $\mathrm{Var}(T_r)$ into pervious and impervious contributions, we use

$$\mathrm{Var}(T_r)_p = \{E[T_r^2]_p + E[T_r]_p^2\} + E[T_r]_p E[T_r]_i \tag{47}$$

and

$$\mathrm{Var}(T_r)_i = \{E[T_r^2]_i + E[T_r]_i^2\} + E[T_r]_p E[T_r]_i, \tag{48}$$

where $\mathrm{Var}(T_r) = \mathrm{Var}(T_r)_p + \mathrm{Var}(T_r)_i$. Equations (47) and (48), in addition to the variance of T_b, are useful because they can quantify the relative contributions from pervious and impervious areas to the hydrograph duration. Additionally, $R_{x,y,t}$ and the variance together can be used as a measure of peakedness, where a large $R_{x,y,t}$ and a small variance would indicate a larger peakedness. The mean runoff time is comparable to a time of concentration, so separating the mean time into pervious and impervious contributions provides a measure of their relative impacts on the time of concentration.

[23] Figure 4a illustrates the estimation of $E[T_r]$ and $E[T_b]$ for both pervious and impervious areas for a range of watershed sizes. The figure shows that pervious areas have a larger mean runoff time than impervious areas and therefore contribute the most to the total mean runoff time. The figure can also help identify the importance of different processes in the runoff time. It shows for the pervious areas how the influence of runoff generation on the mean travel time and variance decreases as the watershed size increases while the routing time becomes more dominant. This ability to distinguish between the contribution of different processes and between pervious and impervious areas is precisely the goal behind the proposed method. For example, for watershed sizes greater than approximately 64 km^2, $E[T_b]_p$ becomes larger than $E[T_r]_p$. To interpret, this means that for locations within the NW Branch watershed with drainage areas greater than 64 km^2 the routing process is the dominant process. Similarly, in Figure 4b, the variance of pervious areas, $\mathrm{Var}(T_r)_p$ and $\mathrm{Var}(T_b)_p$, contribute the most and the importance of processes can vary across the different watershed sizes.

5. Space-Time Relationships for Different Scenarios

[24] We use the relationships obtained in section 4 to examine the impacts from different rainfall and imperviousness scenarios. We first investigate the relationship between the rainfall pattern and imperviousness. We then use different imperviousness scenarios to find how these affect runoff and routing processes.

5.1. Imperviousness and the Space-Time Rainfall Pattern

[25] Because the spatial pattern of rainfall is an important source of space-time variability in urbanized watersheds [*Segond et al.*, 2007], we would like to understand its effects on the proposed relationships. For this comparison we selected three different patterns of rainfall. We used the observed pattern shown in Figure 1a, which is referred to as the actual pattern. The actual pattern has the salient characteristic that most of the rainfall falls on the upstream portion of the watershed, which is also the most pervious section. We inverted the pattern in Figure 1a to have most of the rain fall on the downstream portion of the watershed, where imperviousness is concentrated; this pattern is referred to as the inverted pattern. The inversion was simply done by flipping the actual data along the horizontal and vertical axes passing through the geometric centroid of the watershed. We assumed the third pattern to be equal to the areal average of the actual spatial rainfall pattern; this pattern is referred to as the uniform pattern.

[26] The three rainfall patterns examined indicated that the spatial covariance terms can vary with watershed size and with the form of the spatial rainfall pattern. For example, the term $\mathrm{Cov}[P_t(x,y),I_t(x,y)]$ was found to vary considerably as a function of watershed scale. The changes in $\mathrm{Cov}[P_t(x,y),I_t(x,y)]$ are illustrated in Figure 5. In Figure 5a the actual rainfall pattern produces a $\mathrm{Cov}[P_t(x,y),I_t(x,y)]$ that changes with watershed size and can reach a minimum value of approximately −0.08. Figure 5b shows that when the rainfall is inverted the $\mathrm{Cov}[P_t(x,y),I_t(x,y)]$ varies with watershed size and has instead a positive value, the largest value being approximately 0.05. The significance of these magnitudes can be understood by their role in equation (21). In essence, the values of −0.08 and 0.05 mean the runoff from impervious areas is decreased by 8% or increased by 5% depending on whether the spatial pattern of rainfall coincides with the imperviousness pattern. Obviously when rainfall is assumed uniform this covariance becomes

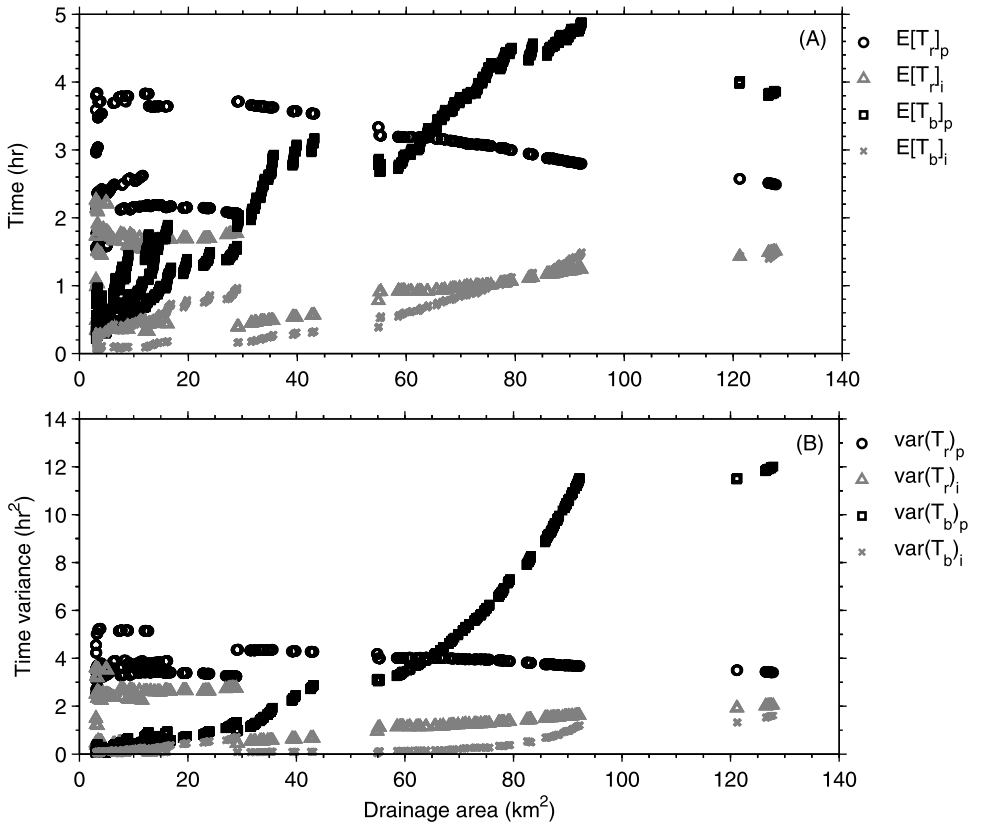

Figure 4. Estimation of the mean runoff time and variance for a range of watershed sizes: (a) mean runoff time for the holding time of the rainfall excess, $E[T_r]$, and routing travel time, $E[T_b]$; (b) variance of the runoff time induced by the rainfall excess, $\mathrm{Var}(T_r)$, and routing, $\mathrm{Var}(T_b)$. The estimates of the mean and variance of the runoff time are separated into pervious and impervious contributions.

essentially zero. The term $\mathrm{Cov}[P_t(x,y),W_t(x,y)]$ was found to be negligible for all the rainfall patterns examined and across the entire range of watershed sizes. This means the rainfall and runoff generation pattern are not acting together in this case to increase or decrease the amount of rainfall excess. A similar finding was reported by *Woods and Sivapalan* [1999] for a nonurbanized watershed.

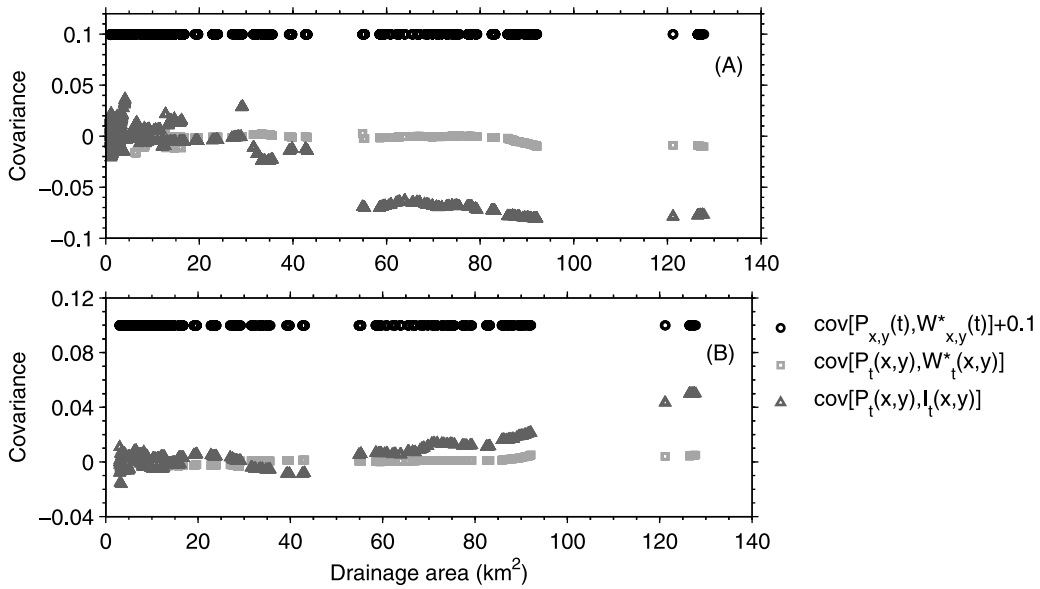

Figure 5. Illustration of the values of $\mathrm{Cov}[P_{x,y}(t),W_{x,y}(t)]$, $\mathrm{Cov}[P_t(x,y),W_t(x,y)]$, and $\mathrm{Cov}[P_t(x,y),I_t(x,y)]$ for a range of watershed sizes and (a) the actual rainfall and (b) the inverted pattern. The values of $\mathrm{Cov}[P_t(x,y),W_t(x,y)]$ have been offset by 0.1 for clarity.

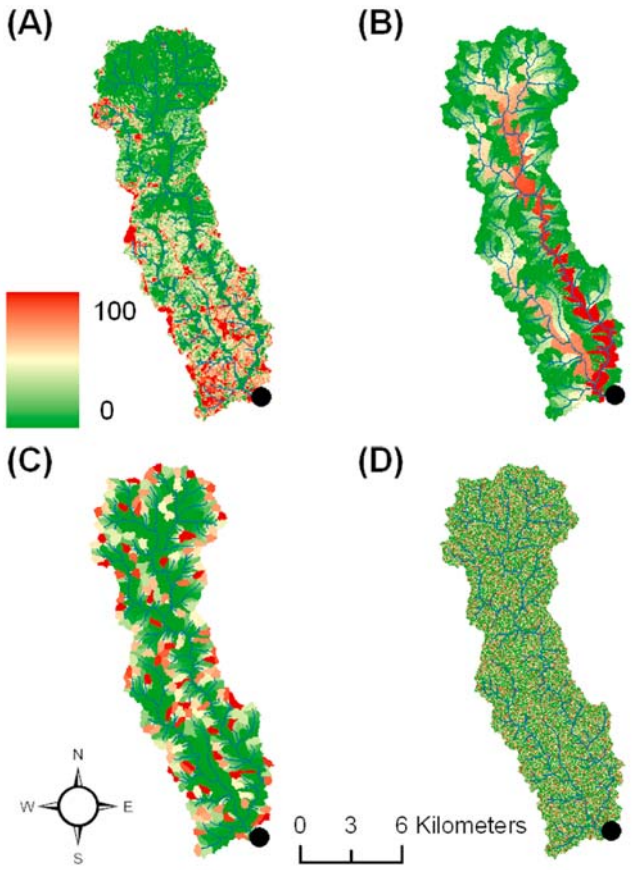

Figure 6. Imperviousness scenarios: (a) actual, (b) channel clustering, (c) source clustering, and (d) random pattern. The scenarios keep the amount of total imperviousness relative to the main outlet the same; only the spatial distribution is varied.

5.2. Imperviousness Scenarios

[27] We also varied the imperviousness pattern to examine its effect on the relationships in section 4. To obtain different imperviousness patterns we used a similar approach to the one by *Mejía and Moglen* [2009]. The approach allows the simulation of distinct imperviousness scenarios. These scenarios are illustrated in Figure 6 and they represent extreme ways of organizing imperviousness within the watershed. The patterns in Figure 6a, 6b, 6c, and 6d are referred to as current, channel clustering, source clustering, and random, respectively. The patterns keep the amount of total imperviousness relative to the main outlet the same; only the spatial distribution is varied. The current pattern represents actual land use conditions. In the channel clustering pattern, imperviousness is organized along the main channel and this tends to reduce peak flows along the entire stream network as shown by *Mejía and Moglen* [2009]. The source clustering pattern clusters development around source streams, which tends to increase peak flows along the entire network [*Mejía and Moglen*, 2009]. The random pattern represents an extreme form of sprawl where development is randomly distributed across the overall watershed area. These simulated patterns mimic some of the main regularities in observed imperviousness within watersheds [*Poff et al.*, 2006]. *Poff et al.* [2006] found, for example, that in the southwestern United States urbanization tends to be more prevalent on the valley floors and floodplains (like the channel clustering pattern), whereas in the southeast, urbanization is more common on headwater watersheds and around low-order streams (as in the source clustering pattern).

[28] An important effect of the imperviousness scenarios examined was to change the magnitude and sign of Cov $[P_t(x,y),I_t(x,y)]$ across watershed sizes, suggesting a dependence between the form of the imperviousness pattern and the spatial distribution of rainfall. These changes are illustrated in Figure 7. In Figure 7, for the storm event considered, the current scenario produced the largest changes in the magnitude of Cov$[P_t(x,y),I_t(x,y)]$. The sign of Cov$[P_t(x,y),I_t(x,y)]$ for the current and channel clustering scenarios tended to be negative for the larger watershed sizes while this term was positive for the source clustering. As expected, in the random scenario, Cov$[P_t(x,y),I_t(x,y)]$ is approximately zero for all watershed sizes. Thus, the results in Figure 7 show how the importance of the spatial pattern of rainfall can vary depending on the overall imperviousness pattern. This may be useful for deciding in suburban watersheds when to use spatially distributed rainfall in hydrologic modeling.

[29] We also used the relationships in section 4 to estimate the peakedness of a hydrograph. The peakedness in this case is expressed as the ratio of $R_{x,y,t}$ and Var(T_o). A lower value of this ratio indicates low peakedness and the opposite for a higher value because a lower value of $R_{x,y,t}$, the storm runoff, and a larger variance, as a surrogate for the hydrograph duration, would indicate a wider and flatter hydrograph shape. Figure 8 shows the peakedness estimates for the four imperviousness scenarios. The peakedness in Figure 8 was separated into pervious and impervious contributions as a way to quantify the relative importance of the mixed land use conditions on the hydrologic response. The separation was done by using $(R_{x,y,t})_p$, equation (25), and $(R_{x,y,t})_i$, equation (26), divided by the total variance, Var(T_o). The total peakedness (i.e., the sum of the pervious and impervious peakedness) is also plotted in Figure 8. In Figure 8, the main difference in the peakedness of the scenarios appears to be the magnitude of the peakedness. For example, the source clustering scenario in Figure 8c tends to have higher total peakedness than the channel clustering scenario shown in Figure 8b. This observation is more accentuated for the smaller watershed sizes. Also notice the pervious areas contribute the most to the peakedness across the range of watershed sizes and for all four patterns. Normally, peak flows in urbanized watersheds are understood as being dominated by the urban runoff [*Andrieu and Chocat*, 2004], but in the mixed pervious-impervious land use conditions of suburban watersheds this might not be the case as illustrated in Figure 8.

[30] If the peakedness is instead estimated relative to the pervious and impervious values of both $R_{x,y,t}$ and Var(T_o), $(R_{x,y,t})_p$/Var$(T_o)_p$ or $(R_{x,y,t})_i$/Var$(T_o)_i$, other distinctions between the peakedness of the scenarios emerge. These distinctions are illustrated in Figure 9. The main distinction is that the pervious and impervious contributions for the random and source clustering scenarios seem to be equally strong, but in the current and channel clustering scenarios the peakedness from impervious areas is more dominant despite the fact that over the entire watershed the pervious

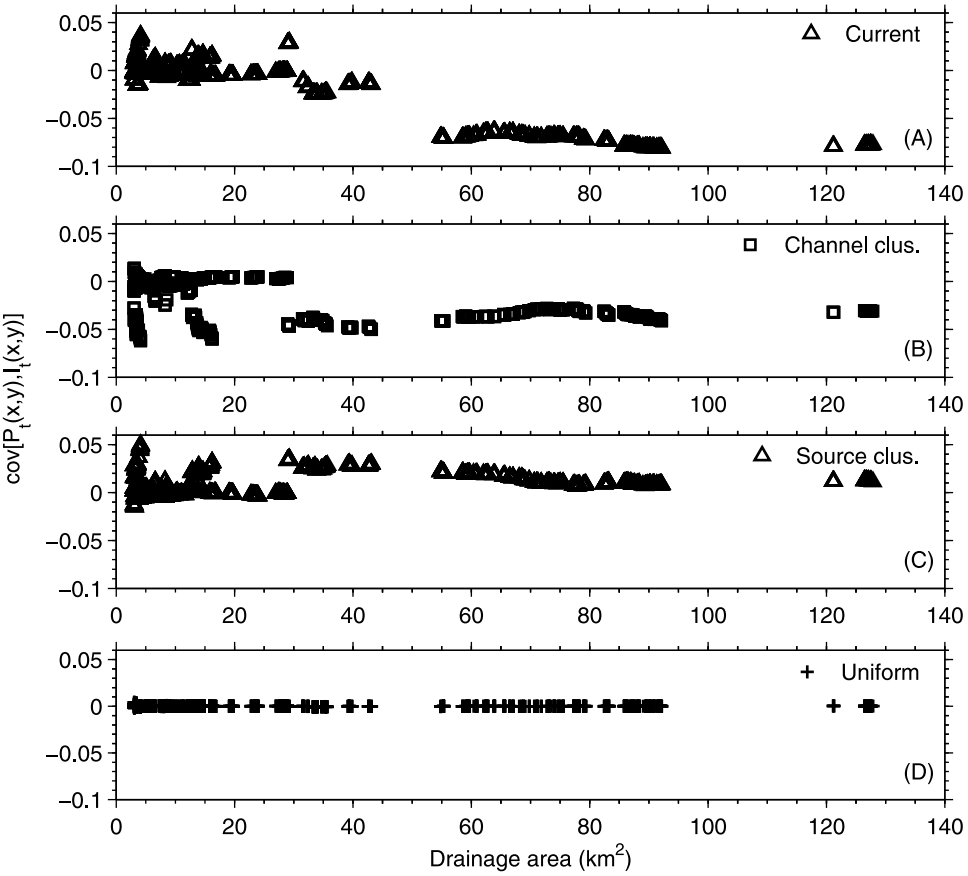

Figure 7. Illustration of the changes in Cov[$P_t(x,y)$,$I_t(x,y)$] for a range of watershed sizes, and the (a) actual, (b) channel clustering, (c) source clustering, and (d) random imperviousness scenarios.

areas are contributing 44% more storm runoff than impervious areas. Interestingly, the current scenario had lower total peakedness in Figure 8, but now the peakedness owing to imperviousness, as shown in Figure 9, is clearly larger than the pervious one. The reason for the dominance of the imperviousness peakedness for the current and channel clustering scenarios in Figure 9 is because these scenarios place imperviousness in locations that are, for this case, prone to soil saturation near the stream channels. This causes a switching of runoff production to impervious areas rather than pervious ones, which has the beneficial consequence of limiting the total amount of runoff, when compared to the total amount of runoff that would be produced if the impervious areas were away from the soil saturated areas. But this can also cause imperviousness to play a larger role on hydrograph variability. The increased role of imperviousness on the peakedness and the proximity to the stream channels can indicate larger disturbances to the flow regime, or greater efficiency in transporting pollutants [*Zhu et al.*, 2008]. Thus, the estimated peakedness can be used to distinguish some of the impacts from imperviousness on streamflows that could be difficult to quantify using other measures.

6. Summary

[31] An analytical method was proposed that relates the spatial distribution of imperviousness in a suburban watershed to the space-time variability of rainfall, runoff generation, and routing. The objective was to separate the pervious and impervious contributions to the different processes and at the same time account for space-time variability. The method is built on an earlier theoretical framework proposed by *Woods and Sivapalan* [1999]. The separation into pervious and impervious contributions was achieved by accounting explicitly for the location of pervious and impervious areas within the watershed. The method was used to obtain various hydrologic relationships and the estimation of the relationships was illustrated with data and conditions for a suburban watershed in the Maryland Piedmont region. Furthermore, the method and derived relationships were used to investigate several scenarios with emphasis placed on the imperviousness pattern.

[32] Our application in the Maryland Piedmont indicated the spatial pattern of runoff generation and rainfall have a negligible relationship during wet conditions, when the runoff pattern from excess saturation is most prevalent. We found the relationship between rainfall and the imperviousness pattern can be important and can vary depending on the spatial pattern of both rainfall and imperviousness. The relationship was quantified using the covariance between the rainfall and imperviousness pattern. This covariance suggested that when most of the rain falls on a highly urbanized section of the watershed the imperviousness becomes more important. The variance of the hydrologic response and the amount of runoff were used to quantify the pervious and impervious contributions to the peakedness of the hydrograph. This analysis indicated that in suburban watersheds with mixed land use conditions the peakedness

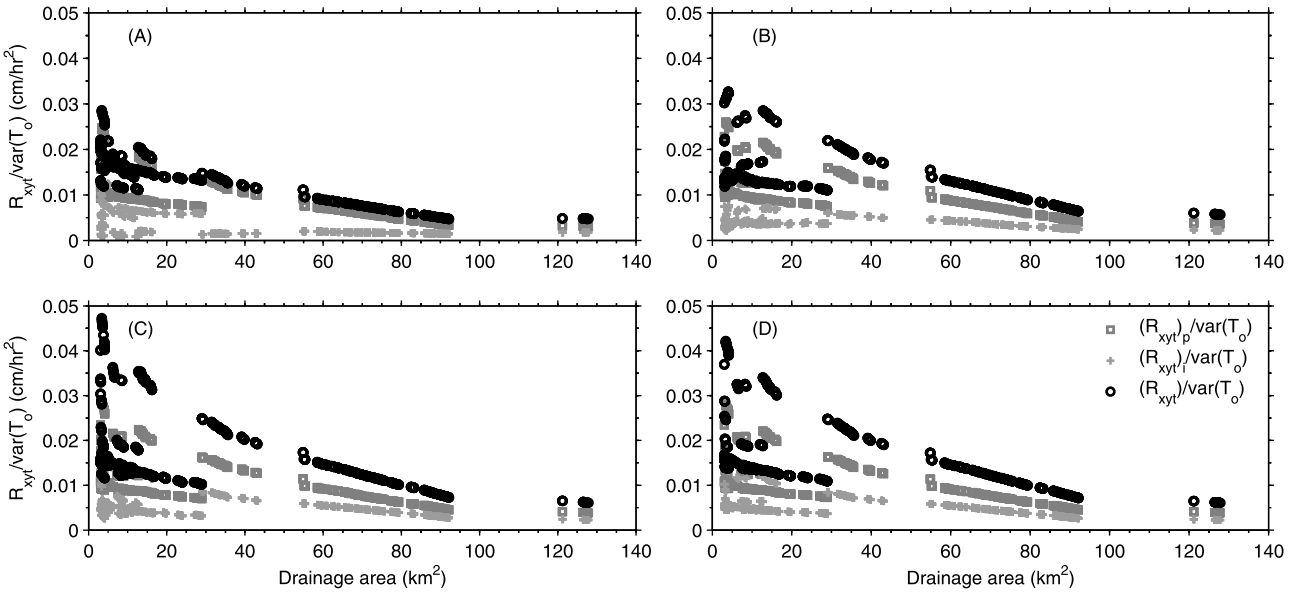

Figure 8. Peakedness for the (a) actual, (b) channel clustering, (c) source clustering, and (d) random imperviousness scenarios. The total peakedness was determined as the ratio of $R_{x,y,t}$ to the total Var(T_o). The pervious and impervious contributions were estimated using $(R_{x,y,t})_p$/Var(T_o) and $(R_{x,y,t})_i$/Var(T_o), respectively.

owing to pervious areas can be greater than that of impervious areas for a range of watershed sizes. It also suggested that in some cases (e.g., the channel clustering imperviousness scenario), even if the amount of runoff from pervious areas is larger, the impervious contribution can have a larger impact than the pervious contribution on the peakedness depending on the overall distribution of imperviousness and the relationship chosen to quantify the peakedness.

[33] The proposed method can be used as an assessment of the importance of various hydrologic processes and sources of space-time variation in a suburban watershed. This could be useful when deciding the level of model complexity or the model components needed to simulate the response of a suburban watershed. The method can also be useful to study how changes in forcing or watershed conditions (e.g., rainfall or land use) may affect runoff or the hydrologic response. Because the method allows the determination of analytical relationships in terms of the different space-time variations in rainfall, runoff, and routing, it can be implemented in a straightforward manner without the necessity of detailed modeling.

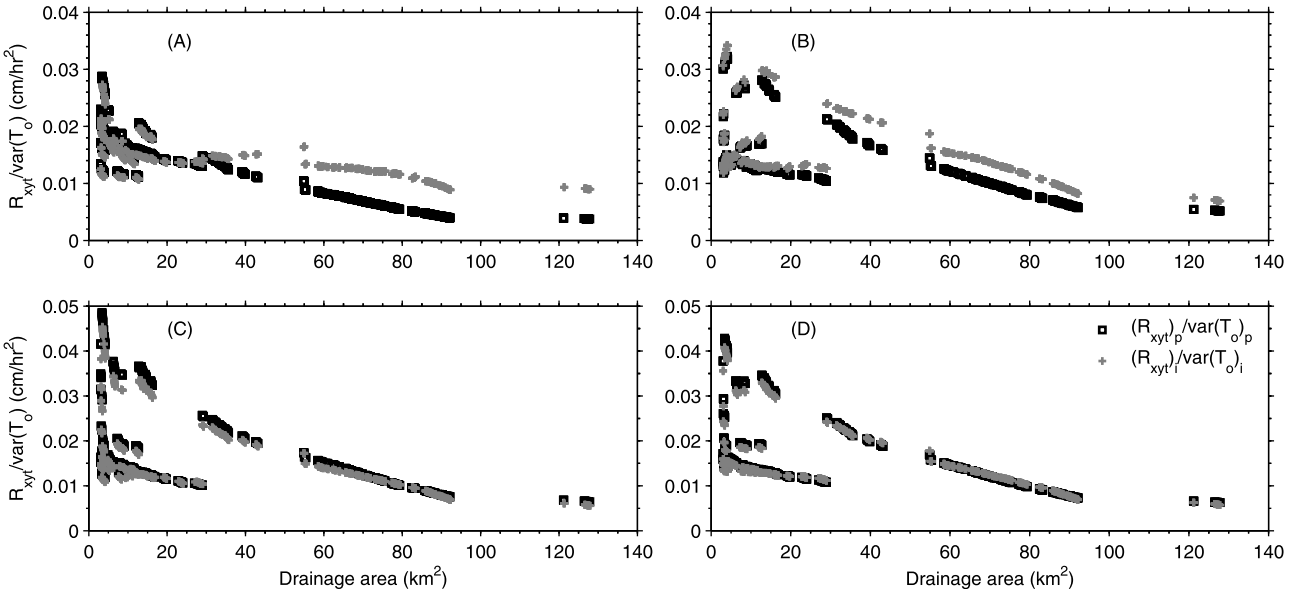

Figure 9. Peakedness for the (a) actual, (b) channel clustering, (c) source clustering, and (d) random imperviousness scenarios. The peakedness of pervious and impervious contributions were estimated using $(R_{x,y,t})_p$/Var$(T_o)_p$ and $(R_{x,y,t})_i$/Var$(T_o)_i$, respectively.

[34] **Acknowledgments.** We gratefully acknowledge the Environmental Protection Agency's support of this project through grant RD83334601. We are also very grateful to the three anonymous reviewers for their detailed comments and constructive suggestions, which helped improve the quality of the manuscript.

References

Anderson, D. G. (1970), Effects of urban development on floods in Northern Virginia, *Professional Paper 2001-C*, pp. C1–C22, U.S. Geol. Surv., Washington, D. C.

Andrieu, H., and B. Chocat (2004), Introduction to the special issue on urban hydrology, *J. Hydrol.*, *299*(3–4), 163–165.

Beven, K. J., and M. J. Kirkby (1979), A physically based variable contributing area model of basin hydrology, *Hydrol. Sci. Bull.*, *24*(1), 43–69.

Carter, R. W. (1961), Magnitude and frequency of floods in suburban areas, *Professional Paper 424-B*, pp. B9–B11, U.S. Geol. Surv., Washington, D. C.

DeFries, R., and K. N. Eshleman (2004), Land-use change and hydrologic processes: A major focus for the future, *Hydrol. Processes*, *18*(11), 2183–2186.

Eagleson, P. S. (1967), A distributed linear model for peak catchment discharge, paper presented at the International Hydrology Symposium, Colo. State Univ., Fort Collins, Colo.

Environmental Protection Agency (EPA) (2004), Protecting water resources with smart growth, *Rep. EPA-231-R-04-002*, 120 pp., Washington, D. C.

Grayson, R. B., I. Moore, and T. McMahon (1992), Physically based hydrologic modeling 2. Is the concept realistic? *Water Resour. Res.*, *28*(10), 2659–2666, doi:10.1029/92WR01259.

Homer, C., J. Dewitz, J. Fry, M. Coan, N. Hossain, C. Larson, N. Herold, A. McKerrow, J. N. VanDriel, and J. Wickham (2007), Completion of the 2001 National Land Cover Database for the conterminous United States, *Photogramm. Eng. Remote Sens.*, *73*(4), 337–341.

Hundecha, Y., and A. Bárdossy (2004), Modeling of the effect of land use changes on the runoff generation of a river basin through parameter regionalization of a watershed model, *J. Hydrol.*, *292*(1–4), 281–295.

Irwin, E. G., and N. E. Bockstael (2007), The evolution of urban sprawl: Evidence of spatial heterogeneity and increasing land fragmentation, *Proc. Natl. Acad. Sci. U. S. A.*, *104*, 20,672–20,677, doi:10.1073/pnas.0705527105.

Johnson, M. P. (2001), Environmental impacts of urban sprawl: A survey of the literature and proposed research agenda, *Environ. Plann. A*, *33*(4), 717–735.

Leopold, L. B. (1968), Hydrology for urban land planning: A guidebook on the hydrologic effects of urban land use, in *U.S. Geol. Surv. Circ. 554*, 18 pp., U.S. Geol. Surv., Reston, Va.

McCuen, R. H. (2003), Smart growth: Hydrologic perspective, *J. Prof. Issues Eng. Educ. Pract.*, *129*(151), doi:10.1061/(ASCE)1052-3928(2003)129:3(151).

Mejía, A. I. (2009), The spatial distribution of imperviousness in watershed hydrology, Ph.D. dissertation, 155 pp., Univ. of Md. at College Park.

Mejía, A. I., and G. E. Moglen (2009), Spatial patterns of urban development from optimization of flood peaks and imperviousness-based measures, *J. Hydrol. Eng.*, *14*(4), 416–424.

Menabde, M., and M. Sivapalan (2001), Linking space-time variability of river runoff and rainfall fields: A dynamic approach, *Adv. Water Resour.*, *24*(9–10), 1001–1014, doi:10.1016/S0309-1708(01)00038-0.

Mesa, O. J., and E. R. Mifflin (1986), On the relative role of hillslope and network geometry in hydrologic response, in *Scale Problems in Hydrology*, edited by V. K. Gupta et al., pp. 1–17, D. Reidel, Norwell, Mass.

Moglen, G. E. (2009), Hydrology and impervious areas, *J. Hydrol. Eng.*, *14*(4), 303–304, doi:10.1061/(ASCE)1084-0699(2009)14:4(303).

Morgan, R. P., and S. F. Cushman (2005), Urbanization effects on stream fish assemblages in Maryland, USA, *J. North Am. Benthol. Soc.*, *24*(3), 643–655.

Moussa, R. (2008), Effect of channel network topology, basin segmentation and rainfall spatial distribution on the geomorphologic instantaneous unit hydrograph transfer function, *Hydrol. Processes*, *22*(3), 395–419.

Naef, F., S. Scherrer, and M. Weiler (2002), A process based assessment of the potential to reduce flood runoff by land use change, *J. Hydrol.*, *267*(1–2), 74–79.

National Oceanic and Atmospheric Administration (NOAA) (2008), MARFC Operational NEXRAD Stage III Data, http://dipper.nws.noaa.gov/hdsb/data/nexrad/marfc_stageiii.php, Silver Spring, Md.

National Resources Conservation Service (NRCS) (1986), Urban hydrology for small watersheds, *Tech. Release 55*, Washington, D. C.

National Weather Service (NWS) (1961), Rainfall frequency atlas of the United States, *Tech. Paper 40*, U.S. Dept. of Commerce, Washington, D. C.

Nicótina, L., E. Alessi Celegon, A. Rinaldo, and M. Marani (2008), On the impact of rainfall patterns on the hydrologic response, *Water Resour. Res.*, *44*, W12401, doi:10.1029/2007WR006654.

Niehoff, D., U. Fritsch, and A. Bronstert (2002), Land-use impacts on storm-runoff generation: Scenarios of land-use change and simulation of hydrological response in a meso-scale catchment in SW-Germany, *J. Hydrol.*, *267*(1–2), 80–93.

Olivera, F., and D. Maidment (1999), Geographic Information Systems (GIS)-based spatially distributed model for runoff routing, *Water Resour. Res.*, *35*(4), 1155–1164, doi:10.1029/1998WR900104.

Philip, J. R. (1960), The theory of infiltration, in *Advances in Hydroscience*, edited by V. T. Chow, vol. 5, pp. 215–296, Academic, Orlando, Fla.

Poff, N. L., B. P. Bledsoe, and C. O. Cuhaciyan (2006), Hydrologic variation with land use across the contiguous United States: Geomorphic and ecological consequences for stream ecosystems, *Geomorphology*, *79*(3–4), 264–285.

Rinaldo, A., and I. Rodríguez-Iturbe (1996), Geomorphological theory of the hydrological response, *Hydrol. Processes*, *10*(6), 803–829.

Rinaldo, A., A. Marani, and R. Rigon (1991), Geomorphological dispersion, *Water Resour. Res.*, *27*(4), 513–525.

Rodríguez-Iturbe, I., and A. Rinaldo (1997), *Fractal River Basins: Chance and Self-Organization*, 564 pp., Cambridge Univ. Press, New York.

Rodríguez-Iturbe, I., and J. B. Valdés (1979), The geomorphologic structure of the hydrologic response, *Water Resour. Res.*, *15*(6), 1409–1420.

Saco, P. M., and P. Kumar (2002), Kinematic dispersion in stream networks 1. Coupling hydraulic and network geometry, *Water Resour. Res.*, *38*(11), 1244, doi:10.1029/2001WR000695.

Saco, P. M., and P. Kumar (2004), Kinematic dispersion effects of hillslope velocities, *Water Resour. Res.*, *40*, W01301, doi:10.1029/2003WR002024.

Schueler, T. (1994), The importance of imperviousness, *Watershed Prot. Tech.*, *1*(3), 100–111.

Segond, M. L., H. S. Wheater, and C. Onof (2007), The significance of spatial rainfall representation for flood runoff estimation: A numerical evaluation based on the Lee catchment, UK, *J. Hydrol.*, *347*(1–2), 116–131, doi:10.1016/j.jhydrol.2007.09.040.

Sivapalan, M., and E. F. Wood (1987), A multidimensional model of non-stationary space-time rainfall at the catchment scale, *Water Resour. Res.*, *23*(7), 1289–1299.

Smith, J. A., M. L. Baeck, K. L. Meierdiercks, P. A. Nelson, A. J. Miller, and E. J. Holland (2005), Field studies of the storm event hydrologic response in an urbanizing watershed, *Water Resour. Res.*, *41*, W10413, doi:10.1029/2004WR003712.

Troch, P. A., J. A. Smith, E. F. Wood, and F. P. de Troch (1994), Hydrologic controls of large floods in a small basin, *J. Hydrol.*, *156*(1–4), 285–309.

U.S. Environmental Protection Agency (EPA) (2006), Protecting water resources with higher-density development, *Rep. EPA-231-R-06-001*, 38 pp., Washington, D. C.

U.S. Geological Survey (USGS) (2008a), National Elevation Dataset, http://gisdata.usgs.net/ned/, Reston, Va.

U.S. Geological Survey (USGS) (2008b), National Land Cover Database 2001, http://www.mrlc.gov/index.asp, Reston, Va.

Walsh, C. J., A. H. Roy, J. W. Feminella, P. D. Cottingham, P. M. Groffman, and R. P. Morgan II (2005), The urban stream syndrome: Current knowledge and the search for a cure, *J. North Am. Benthol. Soc.*, *24*(3), 706–723.

Woods, R., and M. Sivapalan (1999), A synthesis of space-time variability in storm response: Rainfall, runoff generation, and routing, *Water Resour. Res.*, *35*(8), 2469–2485, doi:10.1029/1999WR900014.

Zhu, W., J. G. Graney, and K. Salvage (2008), Land-use impact on water pollution: Elevated pollutant input and reduced pollutant retention, *J. Contemporary Water Res. Educ.*, *138*, 15–21.

A. I. Mejía, Department of Civil and Environmental Engineering, University of Maryland, College Park, MD 20742, USA. (aimejia@umd.edu)

G. E. Moglen, The Charles E. Via, Jr. Department of Civil and Environmental Engineering, Virginia Tech, Room 424, Northern Virginia Center, Falls Church, VA 22043, USA. (moglen@vt.edu)